

## Effect of Ageing on Martensitic Transformation in CuZn and CuZnSn Alloys.

J. Dutkiewicz and J. Morgiel

Institute for Metals Research, Polish Academy of Science, Krakow, Poland.

### Introduction.

The characteristic temperatures of martensitic transformation in copper based alloys are very sensitive to ageing due to instability of the  $\beta$  phase at temperatures up to a few hundreds degrees. However, a lot of applications require constant parameters from alloys designed to work at ambient and slightly higher temperatures. In spite of importance of this problem only a few papers were published until now and even the results concerning the best known CuZnAl system are far from consistence. Initial ageing of CuZnAl usually leads to increase in DO<sub>3</sub> ordering and shifts the martensitic transformation to slightly higher temperatures [1,2]. Longer annealing may cause either  $\alpha$  bainite [3,5,10] or  $\gamma$  phase [4] precipitation. They were found to affect the martensite transformation in an opposite way, i.e. by lowering and rising the  $M_s$  temperature respectively. The limited correlation between structure observations and characteristic martensitic temperatures measurements precluded proposing a mechanism responsible for that phenomena.

The aim of the present paper is to study the influence of tin addition on the martensitic transformation temperatures after low temperature ageing, as well as to explain their changes through parallel structure observation. Tin was chosen as a third element in brasses, because of ability of these alloys to withstand high number of thermal transformation cycles without any changes in characteristic temperatures [5].

### Experimental procedure.

The CuZn and CuZnSn alloys were melted from a high purity elements under layer of borax. The composition of alloys as ascertained by chemical analysis, quenching [ $T_q$ ] and martensitic start [ $M_s$ ] temperatures are given in table 1.

Alloy	Composition [wt%]			$T_q$ [°C]	$M_s$ [°C]
	Cu	Zn	Sn		
A	59.6	40.4	-	850	-60
B	62.1	35.3	2.6	830	-20
C	61.2	33.0	5.8	810	-100
D	64.5	25.0	10.5	760	-120
E	65.8	23.7	10.5	770	-15

Table 1: Chemical composition,  $T_q$  and  $M_s$  temperatures of investigated alloy.

The characteristic transformation temperatures were estimated using electrical resistivity measurements with stabilized current source and x-y recording. The structure observations were performed using analytical transmission electron microscope Philips EM 301. Thin foils were prepared using double jet electropolishing in orthophosphoric acid saturated with chromium oxide.

### Results and discussion.

Fig.1 shows electrical resistivity hysteresis loops obtained from alloy C. The samples, in the form of 0.5mm thick strips, were quenched in water at room temperature (quenching rate  $\approx 1500^\circ\text{C}$ ) and aged at  $200^\circ\text{C}$  for different times. It can be seen, that during the first 20 cycles (Fig.1a) no marked shifts in  $M_s$  temperatures occur. This observation confirms a good stability of characteristic temperatures in CuZnSn alloys with respect to thermal cycling [5]. During ageing at  $200^\circ\text{C}$  the  $M_s$  temperature falls down. Longer ageing causes also gradual flattening of the recorded loops, what means, that less and less material undergoes

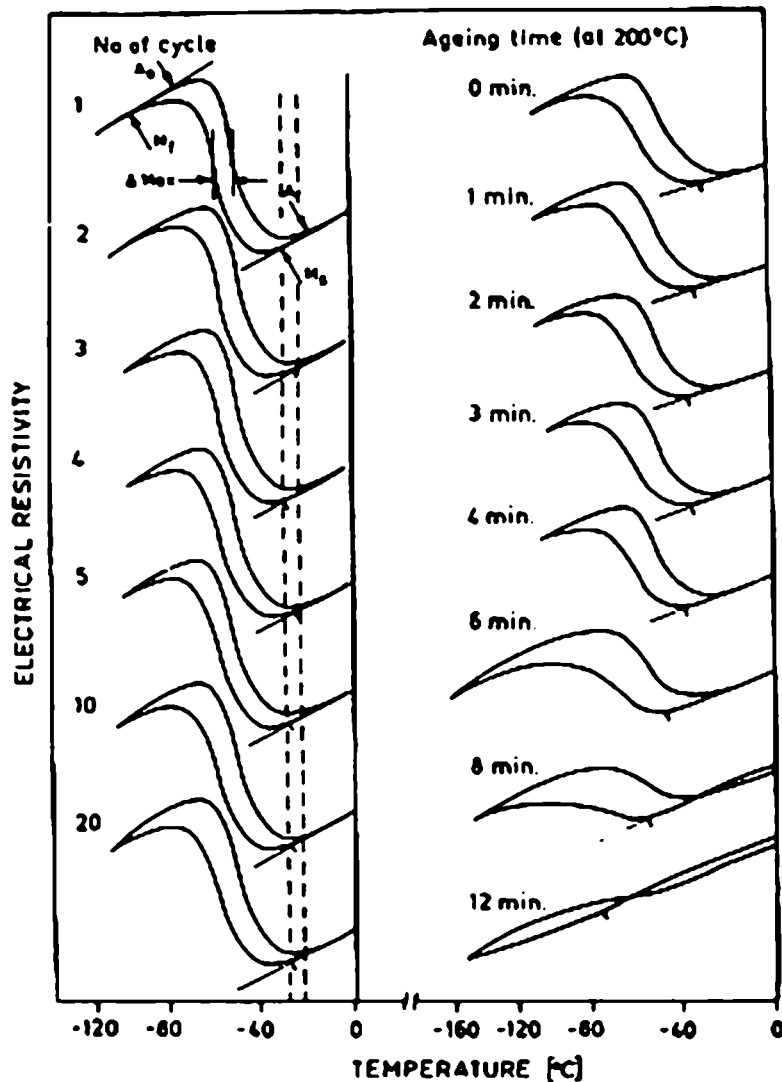


Fig. 1: Electrical resistivity hysteresis loops of alloy C. a) after marked number of cycles, b) after ageing at  $200^\circ\text{C}$ .

the martensitic transformation. The same behavior was observed in all remaining similarly quenched alloys (A-E). When the quenching rate was increased (up to  $15000^{\circ}\text{C}/\text{sec}$ ) by using thinner specimens and cooler quenching bath ( $-10^{\circ}\text{C}$ ) a small increase of  $M_s$  temperatures was recorded (Fig. 2). Then, they fall down, as in the case of alloys quenched in RT water. Only the CuZn alloy does not show increase of  $M_s$  with changed quenching conditions. In order to explain the reason of observed phenomena the transmission electron microscopy investigations were performed. It turned out that the B2 ordered domains always increase significantly with ageing time at  $200^{\circ}\text{C}$ . In alloys B and C, with low tin content, only weak DOs superlattice reflections were present after quenching. In alloys D and E, with 10 wt%Sn, the DOs superlattice reflections are much stronger and the corresponding antiphase domains begin to form (Fig. 3c). After longer ageing time the B2 domains grow (Fig. 3d), while DOs transform from partial into a long range order. It was found, that the increase in the  $M_s$  temperature during initial stages of ageing is closely correlated with the discussed above development in DOs ordering. The above observations are consistent with results obtained for CuZnAl alloys[6]. Next set of microstructures (Fig. 4a,b) show tweed like structure of matrix and  $\gamma$  precipitates at the grain boundaries. Presence of modulated structure, unchanged near grain boundary, may be an indication of spinodal ordering as suggested by Higgins et al.[7] for Fe-Be alloys. The absence of side bands is also justified, because at so large modulation wavelength they are rather included in the fundamental reflections. After longer ageing the antiphase DOs domains grow up into periodically arranged short rods, as shown in Fig.3. The existence of mixture of both B2 and DOs ordering areas was also inferred from Mossbauer spectroscopy measurements [8]. Finally, the formation of  $\gamma$  phase precipitates within the tin rich DOs domains in the final stage of ageing also corroborates the diffusion controlled nature of the modulation discussed at the beginning of

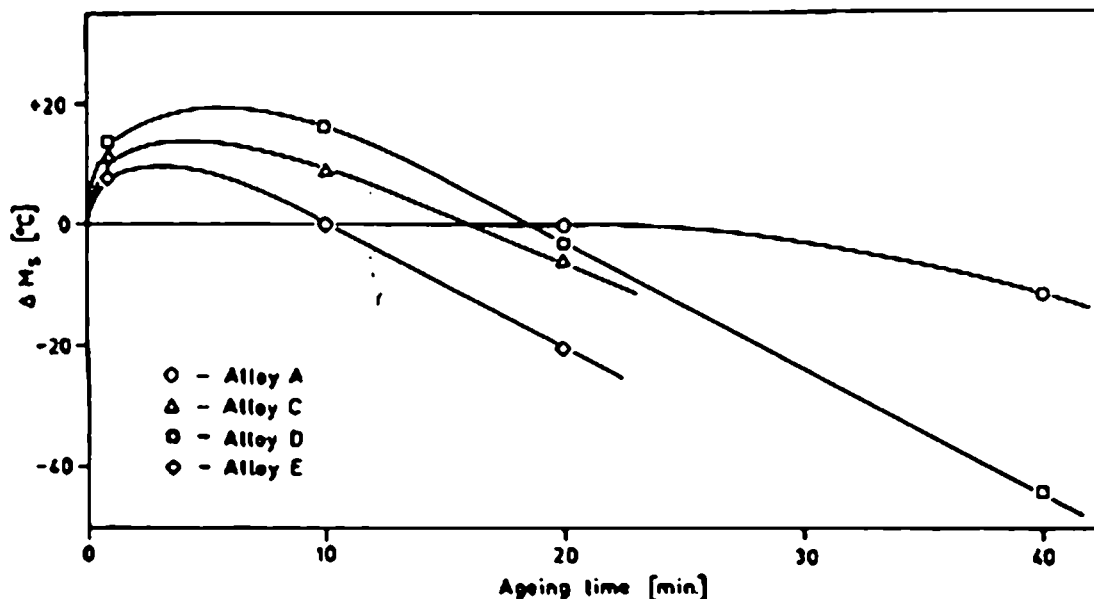
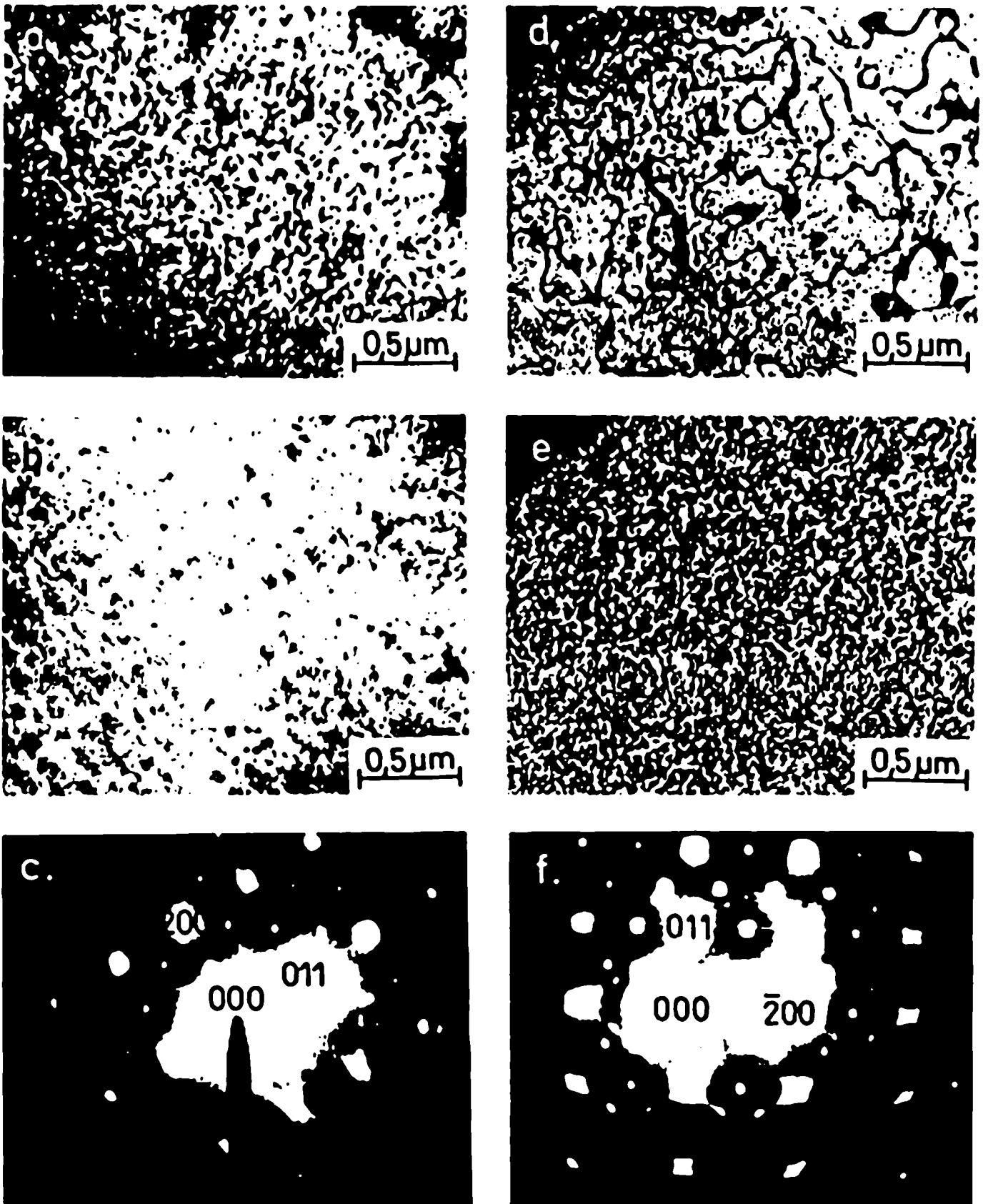


Fig. 2:  $M_s$  temperat. vs ageing time at  $200^{\circ}\text{C}$  for alloys A, B, C, D.



**Fig. 3:** Set of transmission electron microstructures and selected area diffraction pattern (SADP) of alloy D: (a-c) quenched in bath at  $-10^{\circ}\text{C}$ , (d-f) aged at  $200^{\circ}\text{C}$  for 10 min.. a, b dark field (DF) micrographs using  $\{100\}$ , (b, e) DF micrographs using  $\{1/2\ 1/2\ 1/2\}$  spots.

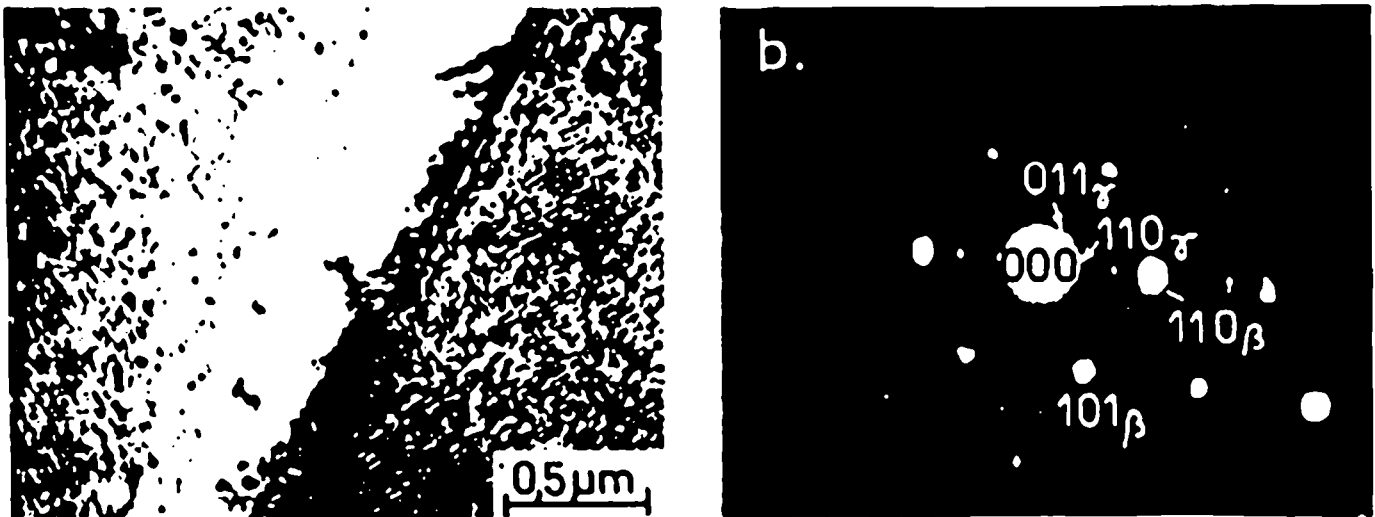


Fig. 4: Alloy D aged 20 min at 200°C. a) BF micrograph, b) SADP.

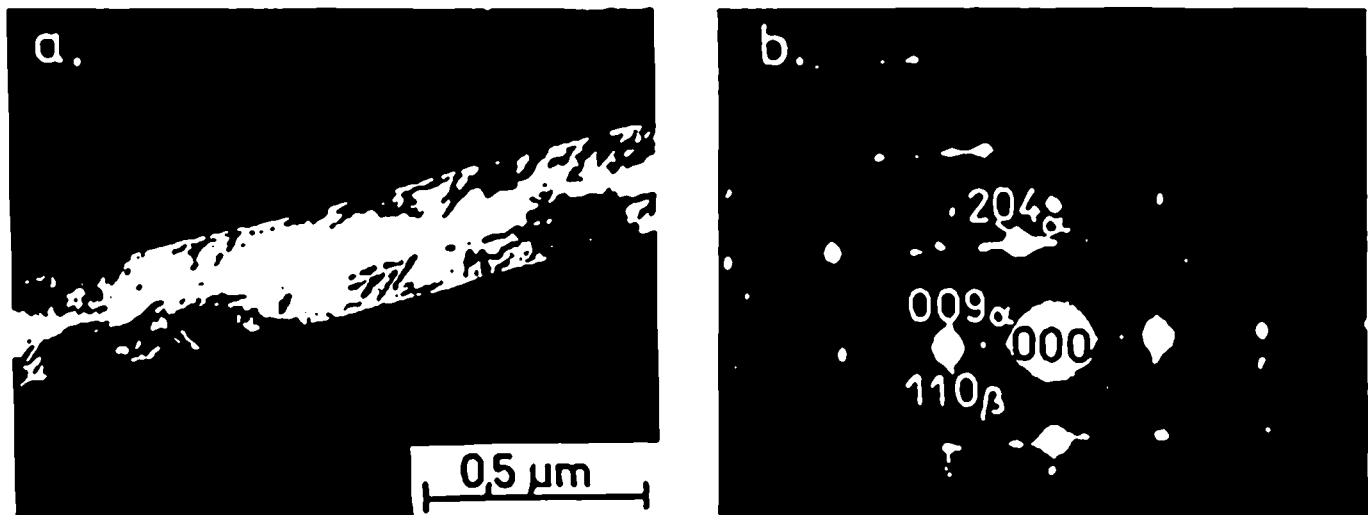


Fig. 5: Alloy C aged 40 min. at 200°C. a) DF micrograph using (204)9R reflection, b) SADP showing  $\beta$  and 9R bainite reflections

this paragraph, and not the existence of a static displacement waves as suggested for CuZnAl alloys [9].

Even before the onset of the  $\gamma$  phase precipitation, the formation of  $\alpha$  bainite plates can be observed. The bainite has the same 9R structure and crystallographic relationship as martensite with the parent  $\beta$  phase. Contrary to a martensite plates, the edges of bainite plates are not straight but show bulging due to diffusion nature of their growth.

After longer ageing time the  $\gamma$  phase starts to precipitate also at a matrix/bainite interfaces. The x-ray spectra obtained from bainite,  $\gamma$  phase and matrix (from the places marked in the micrograph) show a significant difference in tin concentration. Comparison of the Sn  $L\alpha$  intensities shows, that the concentration of tin within bainite is no higher than 8.1 wt%, within  $\gamma$  phase is up to 21 wt%, and 10.5 wt% in the matrix. The zinc concentration varies to much less extent, i.e. in the bainite it is decreased from 33 to 31 wt%. The similar tendency

was observed in other alloys, also those with smaller tin content. Comparing these results to those of Wu and Wayman [10] for CuZnAl alloys, where segregation of aluminum in the bainite was less pronounced than that of zinc, it can be presumed that contrary to aluminum the migration of tin inhibits the zinc segregation out of bainite.

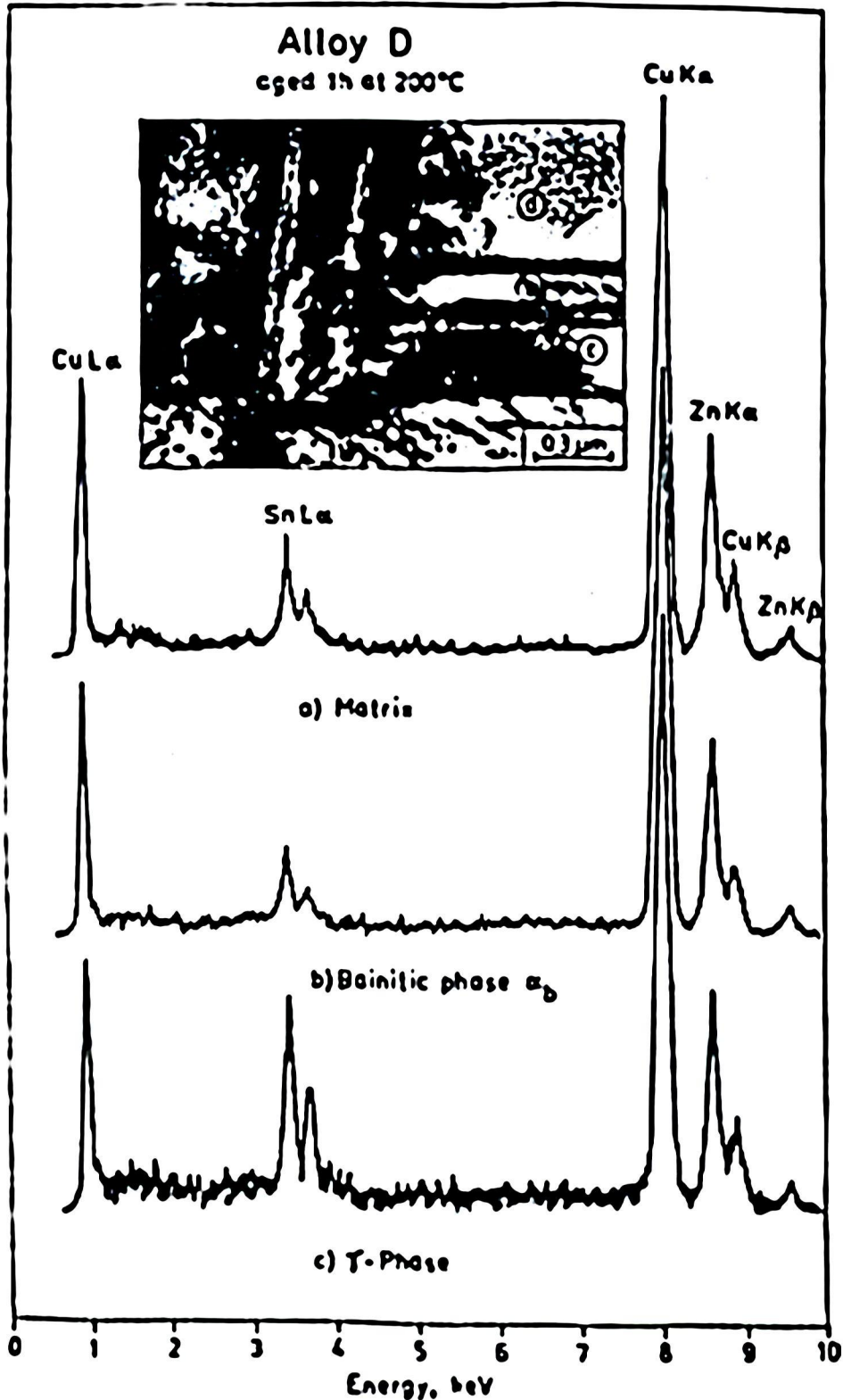


**Fig .6:** TEM microstructure of alloy D aged 1h at 200°C and corresponding x-ray spectra from a-matrix, b-bainite, c- $\gamma$  phase.

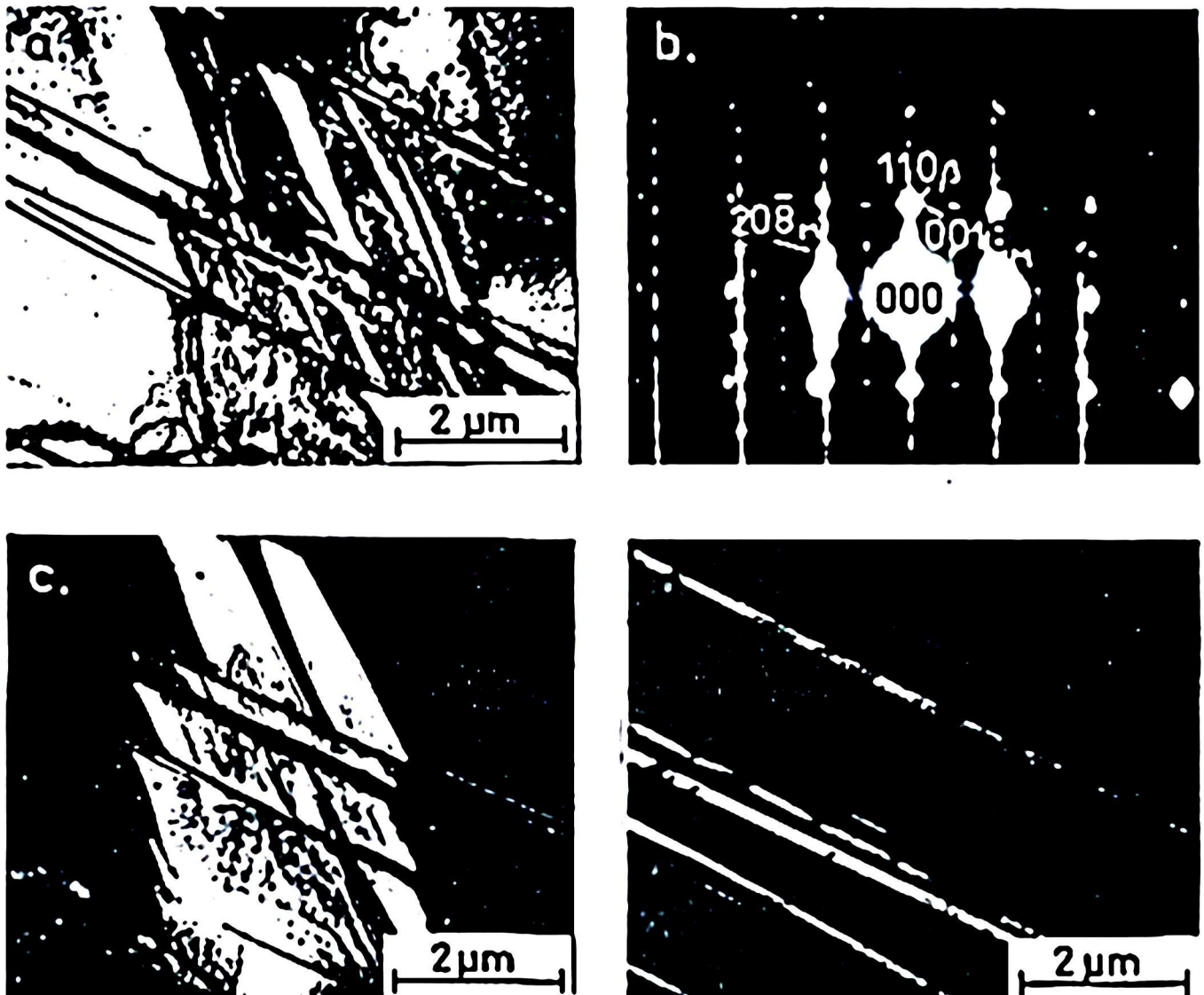


**Fig. 7:** Set of TEM microstructures of alloy C cooled in-situ up to  $-140^{\circ}\text{C}$ . a) BF micrograph. b) SADP with marked  $(208)18R$  bartenite spot. c) DF micrograph taken using  $(208)18R$  spot. d) DF micrograph taken using  $(205)9R$  spot visible in tilted position.

Fig.7 shows martenitic plates formed during in-situ cooling experiment of alloy C, aged previously for 10 min at  $200^{\circ}\text{C}$ . It can be seen, that after cooling down to  $-140^{\circ}\text{C}$  the martenitic plates grow in width, since their length is limited by bainitic needles. The martenite possess  $M18R$  structure and share the same crystallographic relationship with matrix as bainite  $[010]_{\beta} \parallel [110]_{\alpha}$  (Fig.7b). In that way, the lowering of  $M_s$  temperature during later stages of ageing may be attributed to exhaustion of places favoring activity of shear mechanism by previously formed bainite plates. The segregation of tin and zinc at their boundaries further restraining the martenite formation in brass based alloys.

### Conclusions

1. Ageing of the CuZnSn alloys containing more than 5.8wt% tin causes nucleation and growth of the DO<sub>8</sub> antiphase domains elongated in <100> direction. Simultaneously a marked increase in the B2 domains size is observed.
2. The increase of DO<sub>8</sub> ordering in CuZnSn alloys during first stages of ageing raises the M<sub>s</sub> temperature up to 20°C.
3. Longer ageing time at 200°C induces formation of bainitic plates of 9R structure with frequent stacking faults. Then the  $\gamma$  phase starts to precipitate at the sides of bainitic plates and within tin rich modulations in the matrix.
4. The comparison of the x-ray spectra taken from bainite,  $\gamma$  phase and matrix shows that, the segregation of tin is much more pronounced, than that of copper and zinc.
5. The formation of bainitic plates causes significant decrease of M<sub>s</sub> temperature due to both exhausting of nucleation sites by bainite and segregation of tin and zinc into matrix.

### References.

- (1) D.Schoefield, A.P.Miodownik, Metals Technology, 4 (1980) 167.
- (2) J.Perkins, Proceedings ICOMAT 1982, p.697.
- (3) E.R.Kutelia, G.I.Gerovadze, Fiz. Met.Metallov.56 (1983) 1152.
- (4) R.Rapacioli, M.Chandrasekaran, Proceedings ICOMAT 1979,p.596.
- (5) Y.Ikai, K.Murakami, K.Mishima, Proceedings ICOMAT 1982,p.703.
- (6) A.Higuchi, K.Suzuki, R.Sugimoto, N.Nakamura, Proceedings ICOMAT 1986, p 886.
- (7) J.Higgins, R.B.Nicolson, P.Wilkes, Acta Met., 22 (1974) 201.
- (8) J.E.Frackowiak, J.Morgiel, J.Dutkiewicz, Proceedings XIII Conf. Applied Crystallography, Katowice 1988, p.314.
- (9) G.Van Tendeloo, M.Chandrasekaran, F.C.Lovey, ref.6, p.868.
- (10) M.H.Wu, C.M.Wayman, ref.9, p.619.